the plant journal

SEB SOCIETY FOR EXPERIMENTAL BIOLOGY

The Plant Journal (2008) **56**, 716–727 doi: 10.1111/j.1365-313X.2008.03630.x

Mechanism of plant eIF4E-mediated resistance against a Carmovirus (*Tombusviridae*): cap-independent translation of a viral RNA controlled *in cis* by an (a)virulence determinant

Verónica Truniger*, Cristina Nieto, Daniel González-Ibeas and Miguel Aranda

Centro de Edafología y Biología Aplicada del Segura (CEBAS), Consejo Superior de Investigaciones Científicas (CSIC), Apdo. Correos 164, 30100 Espinardo, Murcia, Spain

Received 14 May 2008; revised 26 June 2008; accepted 1 July 2008; published online 15 August 2008.
*For correspondence (fax +34 968396213; e-mail truniger@cebas.csic.es).
GenBank accession numbers: EU589616, EU589617, EU589618, EU589619, EU589620, EU589621, EU589622.

Summary

Translation initiation factors are universal determinants of plant susceptibility to RNA viruses, but the underlying mechanisms are poorly understood. Here, we show that a sequence in the 3′ untranslated region (3′-UTR) of a viral genome that is responsible for overcoming plant eIF4E-mediated resistance (virulence determinant) functions as a 3′ cap-independent translational enhancer (3′-CITE). The virus/plant pair studied here is *Melon necrotic spot virus* (MNSV) and melon, for which a recessive resistance controlled by melon eIF4E was previously described. Chimeric viruses between virulent and avirulent isolates enabled us to map the virulence and avirulence determinants to 49 and 26 nucleotides, respectively. The translational efficiency of a *luc* reporter gene flanked by 5′- and 3′-UTRs from virulent, avirulent and chimeric viruses was analysed *in vitro*, in wheatgerm extract, and *in vivo*, in melon protoplasts, showing that: (i) the virulence determinant mediates the efficient cap-independent translation *in vitro* and *in vivo*; (ii) the avirulence determinant was able to promote efficient cap-independent translation *in vitro*, but only when eIF4E from susceptible melon was added *in trans*, and, coherently, only in protoplasts of susceptible melon, but not in the protoplasts of resistant melon; (iii) these activities required the 5′-UTR of MNSV *in cis*. Thus, the virulence and avirulence determinants function as 3′-CITEs. The activity of these 3′-CITEs was host specific, suggesting that an inefficient interaction between the viral 3′-CITE of the avirulent isolate and eIF4E of resistant melon impedes the correct formation of the translation initiation complex at the viral RNA ends, thereby leading to resistance.

Keywords: cap-independent translation, eIF4E, melon, Melon necrotic spot virus, recessive resistance, resistance breaking.

Introduction

Mutations in or loss of host factors required by viruses to complete their infection cycles (susceptibility factors) can generate recessive alleles that confer host resistance (Fraser, 1990, 1999). Almost all known plant genes with natural or induced recessive resistance alleles (Diaz-Pendon *et al.*, 2004) encode eukaryotic translation initiation factors of the 4E (eIF4E) or 4G (eIF4G) families (Robaglia and Caranta, 2006). Most such mutations confer resistance against viruses of the family *Potyviridae*, the genomes of which characteristically possess a 3′-poly(A) tail, and a covalently bound virus-encoded protein (VPg) at the 5′ end. The VPg cistron encodes an avirulence determinant in several potyvirus/host combinations (Ayme *et al.*, 2006; Borgstrom and Johansen, 2001; Moury *et al.*, 2004; Robaglia and Caranta, 2006), and eIF4E/VPg interaction (Kang *et al.*, 2005; Leonard *et al.*, 2000, 2002, 2004; Robaglia and Caranta, 2006; Schaad *et al.*, 2000; Wittmann *et al.*, 1997) may correlate with virus infectivity (Leonard *et al.*, 2000). Nevertheless, the precise resistance mechanisms have yet to be elucidated. One of the few cases of eIF4E-mediated resistance in viruses other than *Potyviridae* is against *Melon necrotic spot virus* (MNSV) in melon (family *Cucurbitaceae*), which is controlled by the *nsv* gene (Coudriet *et al.*, 1981). MNSV is an isometric monopartite plant virus of the family *Tombusviridae* (genus

Carmovirus), which is endemic in cucurbit crops worldwide (Hibi, 1985; Matsuo *et al.*, 1991). The MNSV genome consists of a 4.3-kb single-stranded positive-sense RNA with five known open reading frames (ORFs) (Diaz *et al.*, 2003; Riviere and Rochon, 1990). As for other tombusviruses, the MNSV genome lacks a 3′-poly(A) tail and a 5′-cap (Diaz *et al.*, 2003, 2004). Our group has previously demonstrated that the *nsv* gene corresponds to a melon *eIF4E* (Cm-*eIF4E*) allele coding for a single amino acid substitution conferring resistance (Nieto *et al.*, 2006), and has characterized an isolate of MNSV, MNSV-264, which can overcome the *nsv*-mediated resistance (Diaz *et al.*, 2002). The critical region for overcoming the resistance comprises the 3′-proximal 397 nucleotides (nt) of the MNSV-264 genome, and the *nsv*-mediated resistance acts at the single-cell level (Diaz *et al.*, 2004). All together, these data suggested that translation of viral RNAs could be the key step regulating resistance to MNSV in melon.

Viral mRNAs have evolved numerous mechanisms to recruit the translational machinery of the host, allowing them to compete with its mRNAs and avoid defence mechanisms that act at the level of translation. Only ~20% of known positive-strand RNA viruses have genomic and subgenomic RNAs with the 5′-cap structure and 3′-poly(A) tail that are typical of eukaryotic mRNAs (van Regenmortel *et al.*, 2000), whereas most lack one or both of these features, and often use their 5′ and/or 3′ termini in alternative gene expression strategies (Dreher and Miller, 2006; Kneller *et al.*, 2006). Several plant viruses that are members of the family *Tombusviridae* and the genus *Luteovirus* lack both the cap and poly(A) tail, initiating cap-independent translation at the 5′ end of the viral RNA, with the help of a cap-independent translational enhancer residing within the (3′-UTR), (3′-CITE) (Miller and White, 2006). The best studied 3′-CITE is that of *Barley yellow dwarf virus* (BYDV, family *Luteoviridae*, genus *Luteovirus*) (Wang *et al.*, 1997), which was recently shown to bind eIF4F through its eIF4G subunit (Treder *et al.*, 2008). All other members of the genus *Luteovirus*, and all members of the *Necrovirus* and *Dianthovirus* genera (family *Tombusviridae*), carry a BYDV-like 3′-CITE (Kneller *et al.*, 2006; Shen and Miller, 2004). Other structurally unrelated 3′-CITEs are found within the 3′-UTRs of the *Tombusviridae*, such as *Tomato bushy stunt virus*, *Maize necrotic streak virus*, *Panicum mosaic virus*, *Hibiscus chlorotic ringspot virus* and *Turnip crinkle virus* (TCV) (Miller *et al.*, 2007).

We set out to determine the molecular mechanism of eIF4E-mediated resistance to MNSV. We found that the virulence determinant functions as a 3′-CITE *in vitro*, as well as *in vivo*, whereas the avirulence determinant required *in vitro* complementation *in trans* by eIF4E from susceptible melon to function as a 3′-CITE. In agreement with this result, efficient *in vivo* translation was observed only in susceptible, but not in resistant, melon. Both 3′-CITEs, from the virulent and avirulent isolates, required the presence *in cis* of the 5′-UTR of MNSV for efficient translation to occur. Therefore, eIF4E-mediated resistance to MNSV acts at the level of cap-independent translation, and the ability of an isolate to overcome this resistance depends on its 3′-CITE.

Results

The virulence determinant of MNSV is an RNA sequence

We previously showed that the genetic determinant for the ability to overcome the *nsv*-mediated resistance in melon maps to the 3′ end of the MNSV-264 genomic RNA (Diaz *et al.*, 2004). Within this region, the program ORF-FINDER (NCBI, http://www.ncbi.nlm.nih.gov) predicted an ORF (ORF X) starting with CTG, which was not represented in the same region of avirulent isolates, including MNSV-Mα5. CTG is the next most efficient initiator after ATG in plant cells (Gordon *et al.*, 1992), and is used as an initiation codon for a number of plant RNA viruses (Shirako, 1998). Therefore, ORF X could encode a protein required to overcome *nsv*-mediated resistance. We therefore disrupted ORF X in an infectious clone of MNSV-264 (Diaz *et al.*, 2004) by introducing several stop codons (Figure 1). The phenotypes of the resulting mutants were tested by electroporation of the *in vitro* transcribed RNA into melon protoplasts from

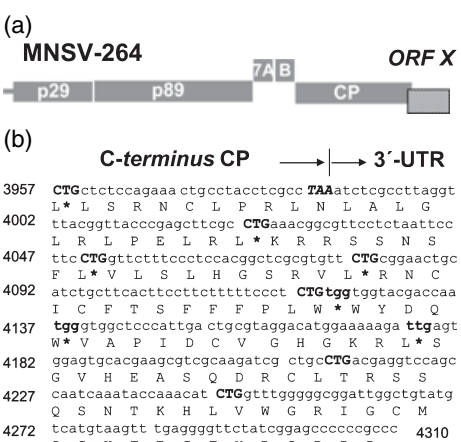

Figure 1. Point mutations that truncate the open reading frame X (ORF X) at the 3′ end of MNSV-264.

(a) Organization of the MNSV genome encoding five proteins. Putative untranslated regions (UTRs) of approximately 80 and 300 nt can be found at the 5′- and 3′-termini, respectively.

(b) Nucleotide sequence of the 3′ end of MNSV-264, which is necessary and sufficient to overcome *nsv*-mediated resistance (Diaz *et al.*, 2004). This includes the last 31 nt, corresponding to the *CP* gene (stop codon indicated in capital letters, italics and bold) and the complete 3′-UTR. Numbers at the left indicate the position of the first nt of each line in the published MNSV-264 sequence (AY330700 in NCBI database). Potential CTG start codons are marked in capital letters and bold. The second CTG is the start codon proposed by the ORF-finder program. An asterisk below codons marked in bold (ctg, ttg or tgg) indicates that they were changed by site-directed mutagenesis into stop codons (tag).

resistant and susceptible varieties, followed by northern blotting. All of the MNSV-264 mutants were able to multiply in resistant melon cells, indicating that the potential ORF X peptide has no role in resistance-breaking. Therefore, we concluded that the 3′ RNA sequence itself, rather than an encoded product, must be the virulence determinant.

To fine-map the virulence determinant, regions from the 3′ end of MNSV-264 genomic RNA were exchanged with those from MNSV-Mα5 to produce reciprocal constructs, using infectious cDNA clones (Diaz *et al.*, 2003, 2004) (Figure 2A). This gave rise to a set of chimeric mutants (Q1–Q7, and the reciprocal Q1*–Q6*) (Figure 2B). The phenotypes of these chimeric mutants were tested as above using protoplasts from susceptible and resistant melons.

The ability of Q1* (in which the entire 3′-UTR of MNSV-Mα5 is replaced by the 3′-UTR of MNSV-264) to multiply in resistant melon protoplasts showed that the virulence determinant was located within the 3′-UTR of MNSV-264. Therefore, all further mutants were constructed with the same genetic background (i.e. the genetic background of MNSV-264), but with chimeric 3′-UTRs, in order to narrow down the location of the virulence determinant within this region. Results showed that Q5 still retained the ability of the parental MNSV-264 to multiply in resistant melons, whereas Q3 did not. Reciprocally, whereas Q5* was unable to multiply in resistant melons, Q2* gained this ability (Figure 2B). These data showed that the sequence (nt 4056–4222) between the exchange positions giving rise to mutants Q2* and Q5* was both sufficient and necessary for resistance-breaking. Significantly, several of the mutants were not viable in susceptible melon cells, suggesting that essential structural requirements had been perturbed.

The virulence determinant is a 49-nt sequence forming part of a stem-loop structure

To reliably predict the secondary structure of the MNSV 3′-UTR, we determined and aligned the sequences of seven new MNSV isolates, and compared them with those available in GenBank (NCBI). As previously reported by Diaz *et al.* (2004), the alignment of all 18 3′-UTRs (see Figure S1) showed that the sequences of MNSV-264 and MNSV-Pα54, the only isolates able to overcome *nsv*-mediated resistance, significantly differed from those of the other isolates (nucleotide identity <50%). We therefore performed separate RNA secondary structure predictions of the 3′-UTRs of virulent and avirulent isolates using RNAALIFOLD (Hofacker *et al.*, 2002). The virulent isolates also included our MNSV-264 mutants constructed to analyse the significance of ORF X (see above), whereas the avirulent isolates included MNSV-Mα5 and the 15 other sequences available in GenBank (Figure 3). Two stem-loop (SL) structures, SL A and SL B, were conserved in both predictions, whereas a third, longer SL structure, which includes the virulence determi-

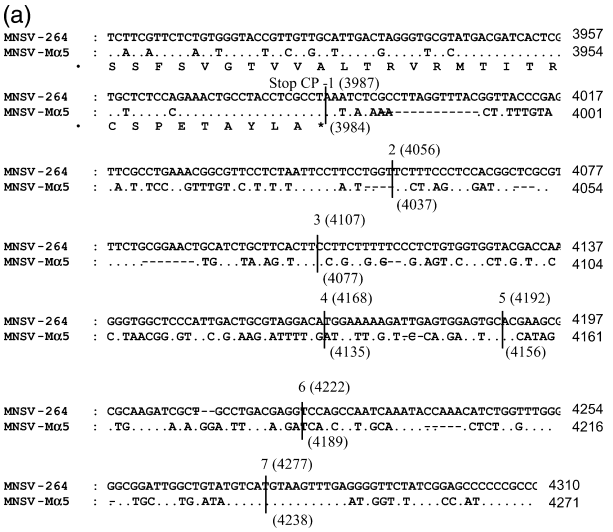

Figure 2. Chimeric mutants used to fine-map the virulence determinant.
(a) Alignment of the nucleotide sequences of the 3′ untranslated regions (3′-UTRs) of MNSV-264 and MNSV-Mα5, and the last 90 nt of the CP gene. Vertical bars (1–7) indicate the exact exchange position (nt numbers given in parentheses) between the two MNSV isolates, leading to the chimeric mutants shown on the right. Numbers at the right indicate the position of the last nt of each line in the published MNSV-264 (AY330700) and MNSV-Mα5 sequences (AY122286).
(b) Scheme showing the exchanges that gave rise to different chimeric mutants. Black segments correspond to MNSV-Mα5, and lined segments correspond to MNSV-264. In the chimeric mutants Q1–Q7, regions of the 3′-UTR of MNSV-264 decreasing in size were exchanged with the corresponding regions from MNSV-Mα5. In the chimeric mutants Q1*–Q5*, regions of the 3′-UTR of MNSV-Mα5 decreasing in size were exchanged with the corresponding regions from MNSV-264. The capacity of these chimeric mutants to multiply (+) or not (−) in susceptible (S) and resistant (R) melon protoplasts, as determined by northern blot, is indicated. Regions critical for virulence are indicated by dashed lines. The phenotype of the chimeric mutants that allowed us to localize the virulence determinant between positions 2 and 5 are marked by a frame.

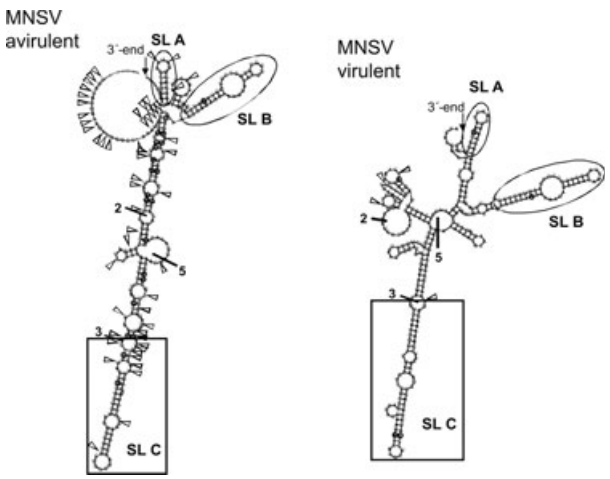

Figure 3. Prediction of RNA secondary structures.
RNA secondary structure predictions were performed with RNAALIFOLD using separate sequence alignments for the 3′ untranslated region (3′-UTR) of MNSV isolates able (MNSV virulent) and unable (MNSV avirulent) to multiply in resistant melon. Differences in nucleotides that maintain the secondary structure are marked with a circle. Three predicted stem loops (SLs) were named A, B and C. SL A includes nt 4286–4304 from MNSV-264 and nt 4247–4265 from MNSV-Mα5. SL B includes nt 4222–4267 from MNSV-264 and nt 4190–4228 from MNSV-Mα5. SL C includes nt 4108–4175 from MNSV-264 and nt 4078–4122 from MNSV-Mα5. Numbers 2, 3 and 5 indicate the exchange positions in the chimeric mutants Q2–Q5. Nucleotide variations that maintain the secondary structure in double-stranded regions because they do not disrupt base-pairing are marked with a circle. Empty arrows point at nucleotide variations located either in double-stranded regions, where they do not support the secondary structure because they disrupt base-pairing, or in single-stranded regions, where they do not affect the secondary structure predicted.

nant region identified above, differed between both structures (Figure 3). Five other secondary structure prediction programs (see Experimental procedures) confirmed the structures predicted by RNAALIFOLD (data not shown). Most nucleotide substitutions occurred in non-paired regions, whereas substitutions in base-paired regions tended not to disrupt base-pairing, or had compensatory mutations in the complementary RNA strand (Figure 3).

Using these predictions, we constructed a new set of chimeric mutants, and tested them by electroporation into protoplasts from susceptible and resistant melon cells, as above. The first exchange comprised SL C (Figure 3), part of the long SL structure that includes the critical sequence identified above. The chimeric mutant Q8, containing the MNSV-264 SL C in a 3′-UTR MNSV-Mα5 background, gained the ability to multiply in resistant melon protoplasts, whereas the reciprocal mutant Q9 lost the resistance-breaking phenotype of its MNSV-264 parent (Figure 4). Therefore, the virulence determinant is located within the 68-nt sequence that forms SL C. The next set of chimeric mutants was constructed to delimit the virulence determinant more precisely. Exchange of the small SL at the end of SL C, resulting in Q10 and Q11, had no effect on the phenotype (Figure 4), indicating that this part of SL C did not contain the entire virulence determinant. As the 19 nt of the terminal SL of SL C of the MNSV-264 and MNSV-Mα5 3′-UTRs are very similar in sequence and structure, it is possible that they are functionally interchangeable. Exchanges of different parts of MNSV-264 SL C with equivalent regions of MNSV-Mα5 (Q12–Q15 in Figure 4) also failed to overcome *nsv*-mediated resistance. Therefore, the virulence determinant must consist of 49 nt, comprising the SL C without the terminal SL (nt 4108–4133 and 4153–4175). On the other hand, the Q16 mutant was not viable, whereas Q15, containing the rest of MNSV-Mα5 SL C, was able to multiply in susceptible melon protoplasts. This suggests that the 26-nt fragment comprised between nt 4078–4089 and 4109–4122 critical for virus multiplication in susceptible melon cells. These 26 nt are highly conserved in the sequences of avirulent MNSV isolates, with only four nucleotide positions changing (see Figure S1). These changes do not affect the secondary structure predicted in Figure 3, as only one is located in a base-paired stem region, and in this case both variations, C and U, are able to base-pair with G.

In conclusion, we have mapped the virulence determinant responsible for breaking *nsv*-dependent resistance to a 49-nt sequence in the 3′-UTR of MNSV-264, and we have identified a 26-nt sequence in the 3′-UTR of MNSV-Mα5 that is required for virus multiplication in susceptible melon cells. Additionally, the viability of nearly all of these chimeric mutants is consistent with the predicted secondary structures of the MNSV-3′-UTRs shown in Figure 3, at least for SL C.

The virulence determinant enhances cap-independent translation efficiency in wheatgerm extract

The genomic RNA of several viruses from the *Tombusviridae* family are uncapped and lack a 3′-poly(A) tail (Hearne *et al.*, 1990; Huang *et al.*, 2000; Miller *et al.*, 2002; Rochon and Tremaine, 1989), and the same is thought to be true for MNSV (Diaz *et al.*, 2003, 2004). To analyse whether a 5′ cap is necessary for MNSV multiplication, virus RNA was transcribed *in vitro* from infectious MNSV cDNA clones in the presence or absence of a cap analogue, and melon cotyledons were mechanically inoculated with the same quantities of capped or uncapped RNA in four separate experiments. Lesion formation was used to measure inoculum infectivity. The number of lesions obtained in resistant melon cotyledons per 10 μg of MNSV-264 RNA was 26 ± 1.2 for uncapped and 24 ± 1.5 for capped RNA. The number of lesions obtained in susceptible melon cotyledons per 10 μg of MNSV-Mα5 RNA was 43 ± 2.3 for uncapped and 46 ± 2.1 for capped RNA. Therefore, inoculation with either capped or uncapped RNA gave rise to equivalent numbers of lesions, suggesting that a cap is not required for translation, and that MNSV genomic RNA is unlikely to be capped.

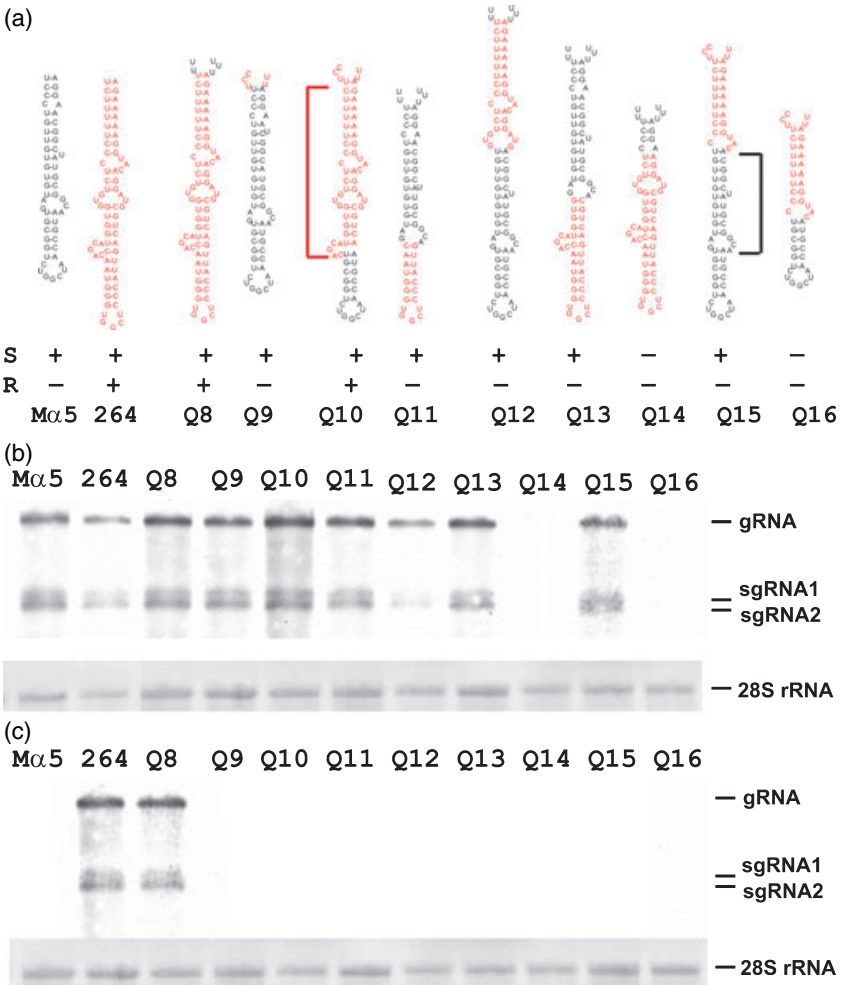

Figure 4. Chimeric mutants based on the RNA secondary structure.
(a) Stem loop C (SL C) of MNSV-Mα5 (black), MNSV-264 (red) and the various chimeric mutants are based on the secondary structure prediction of the 3′ untranslated region (3′-UTR) of MNSV-Mα5 and MNSV-264 (Figure 3). The ability (+) or not (–) of the chimeric mutants to multiply in susceptible (S) or resistant (R) melon protoplasts and plants are indicated. The minimal sequence from MNSV-264 required for resistance breaking is indicated in Q10 by a red bracket, whereas the minimal sequence of MNSV-Mα5 required for viability in susceptible melon is indicated in Q15 by a black bracket.
(b and c) Multiplication of chimeric mutants in susceptible (b) and resistant (c) melon protoplasts as detected by northern blot analysis. Positions of genomic and subgenomic RNAs are indicated. The cRNA probe was synthesized from a full-length MNSV-Mα5 cDNA clone. The amount of total RNA loaded was visualized by methylene blue staining of the 28S rRNA (bottom panels).

The inability of MNSV-Mα5 to multiply in resistant melon protoplasts suggests that translation and/or replication could be affected by *nsv*, although as the *nsv* product is eIF4E, a translation initiation factor, the former case is more likely. To analyse the mechanism, we studied the effect of the 3′-UTR of MNSV on the *in vitro* translational efficiency of a reporter gene. For this purpose, we created chimeric cDNA constructs with the firefly luciferase gene (*fluc*) flanked by the 5′- and 3′-UTRs of MNSV-264 and MNSV-Mα5 in all possible combinations (Figure 5). RNAs from these constructs, obtained by *in vitro* transcription, were translated in wheatgerm extract (WGE), and the relative luciferase activities were then measured (Figure 6). The efficiency of cap-dependent translation, as estimated by the luciferase activity generated by capped RNAs, was high for all constructs, although slightly lower with the MNSV-264 3′-UTR (black bars in Figure 6a). More interestingly, the efficiency of cap-independent translation, as estimated by the luciferase activity generated by uncapped RNAs, was very low for all constructs, except for those with the MNSV-264 3′-UTR together with one of the MNSV 5′-UTRs, which showed a ninefold increase (striped bars in Figure 6a). These results indicate that the MNSV-264 3′-UTR can enhance the cap-independent translation efficiency of a reporter gene in WGE, as long as an MNSV 5′-UTR is also present.

We also tested the translational efficiency of chimeric 3′-UTRs with and without the virulence determinant (mutants Q8 and Q9; see Figure 4). The chimeric 3′-UTR containing the MNSV-264 SL C facilitated the *in vitro* cap-independent translation of the luciferase gene, whereas the chimeric 3′-UTR containing the MNSV-Mα5 SL C did not (Figure 6b). Again, the MNSV 5′-UTR was required for this activity to occur *in cis*. Therefore, the cap-independent *in vitro* translation promoted by the MNSV-264 3′-UTR depends on the *nsv* resistance-breaking determinant.

EIF4E from susceptible melon complements cap-independent translation mediated by the 3′-UTR of the avirulent isolate in WGE

The data reported above show that WGE provides all of the factors required for cap-independent translation mediated

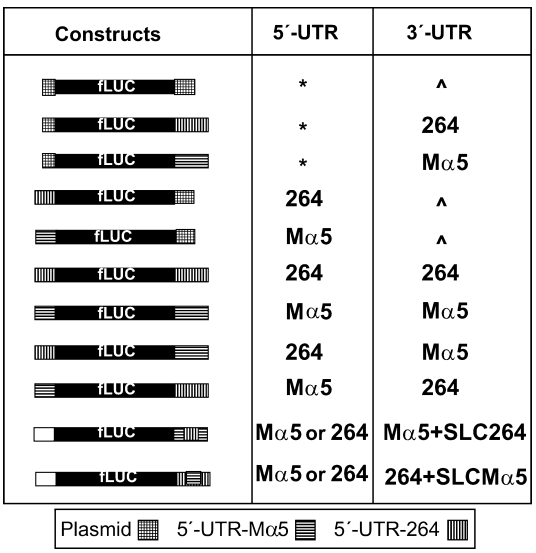

Figure 5. Firefly luciferase constructs with MNSV untranslated regions (UTRs).
The *fluc* gene was flanked with the 5′- and 3′-UTRs of MNSV-Mα5 or MNSV-264 in all possible combinations. The fill-in codes represent the origin of the different sequences flanking *luc*, as indicated in the legend. The RNA transcripts from the constructs labelled with an asterisk (*) contained 38 nt from the plasmid at the 5′ end, and those from constructs labelled with (^) contained 83 nt of the plasmid at the 3′ end.

by the 3′-UTR of MNSV-264, but not of MNSV-Mα5. To determine whether eIF4E from susceptible melon could complement cap-independent translation controlled by the 3′-UTR of MNSV-Mα5, we added purified eIF4E protein (Nieto *et al.*, 2006) to the *in vitro* translation system (Figure 7). Increasing concentrations of purified *Cm*-eIF4ES had no effect on the basal translation efficiency of RNAs with either the 5′- or the 3′-UTR of MNSV-Mα5 (first and second groups of columns in Figure 7). However, if the *luc* gene was flanked by both UTRs, the luciferase activity increased in line with the concentration of *Cm*-eIF4ES (third group of columns in Figure 7), reaching a similar level to that obtained with RNAs flanked by both UTRs of MNSV-264 (fifth group of columns in Figure 7). Therefore the 3′-UTR of MNSV-Mα5 was also able to mediate cap-independent translation initiation *in vitro*, but only in the presence of *Cm*-eIF4ES. As before, this was dependent on the presence of an MNSV 5′-UTR (either isolate) *in cis*. In contrast, eIF4E from resistant melon (*Cm*-eIF4ER), purified in parallel with *Cm*-eIF4ES, was not able to complement the translational efficiency of RNAs controlled by the 3′-UTR of MNSV-Mα5 (fourth group of columns in Figure 7), and neither *Cm*-eIF4ER nor *Cm*-eIF4ES were able to increase the cap-independent translational activity of RNAs controlled by the 3′-UTR of MNSV-264 (fifth group of columns in Figure 7). The chimeric 3′-UTR comprising the MNSV-264 3′-UTR with MNSV-Mα5 SL C (corresponding to the 3′-UTR of Q9; see Figure 4) was also able to enhance cap-independent translation efficiency in the presence of *Cm*-eIF4ES (sixth group of columns in Figure 7). Therefore, SL C from MNSV-Mα5 mediated cap-independent translation *in vitro* in the presence of *Cm*-eIF4ES, whereas it was critical for virus viability *in vivo*.

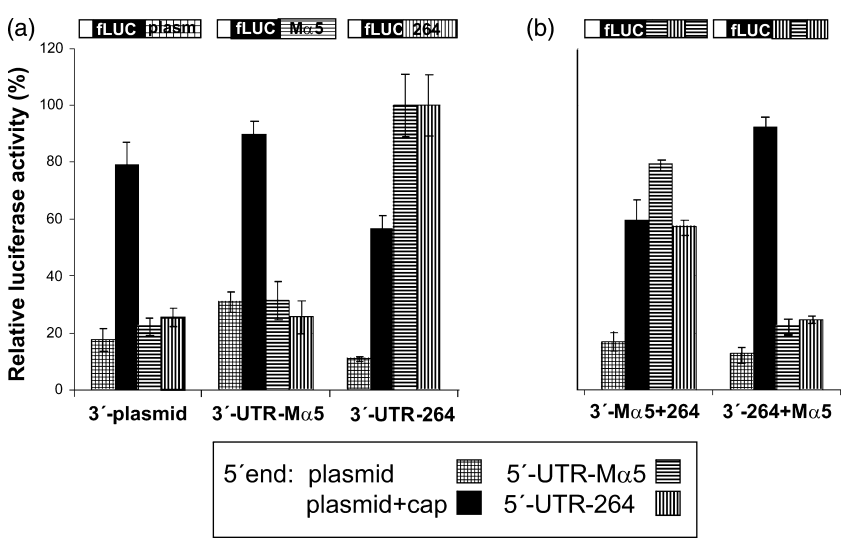

Figure 6. *In vitro* translation of *luc* controlled by 5′ and 3′ untranslated regions (′-UTR) of MNSV.
Firefly luciferase activity generated by *in vitro* translated RNAs from the constructs described above. The *in vitro* transcribed RNAs were translated *in vitro* in wheatgerm extract (WGE), and the translation efficiency was determined by measuring luciferase activity. Relative luciferase activity is represented in the vertical axis (100% corresponds to the activity of 5′-UTR264-*fluc*-3′-UTR264). On the horizontal axis, the grouped bars differ in the sequence at the 3′ end of *fluc*. The fill-in codes of the bars appearing in each group represent different sequences at the 5′ end of *fluc*, as indicated in the legend.
(a) The three groups of constructs contain either no 3′-UTR, the 3′-UTR of MNSV-264 (nt 3988–4310) or the 3′-UTR of MNSV-Mα5 (nt 3985–4271).
(b) The two groups of constructs contain chimeric 3′-UTRs: the group on the left with the 3′-UTR of MNSV-Mα5, with its stem loop C (SL C; nt 4078–4122) exchanged with the SL C sequence of MNSV-264 (nt 4108–4175) required for its resistance-breaking capacity (Q8; Figure 4a), and the group on the right with the 3′-UTR of MNSV-264, with its SL C exchanged with the corresponding SL C of MNSV-Mα5 (Q9, Figure 4a).

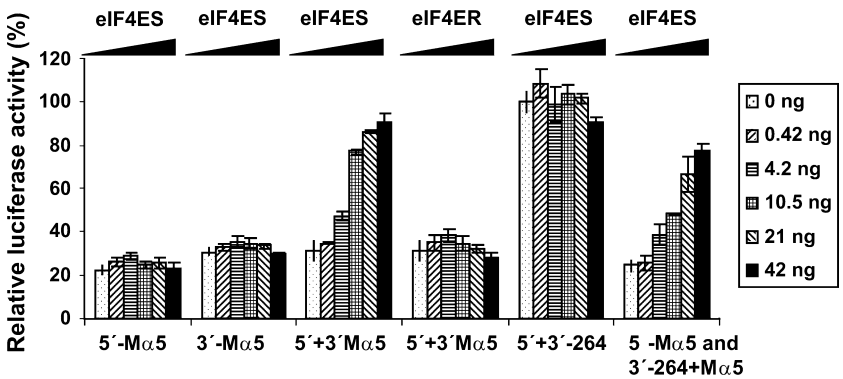

Figure 7. *In vitro* translation of *fluc* controlled by 5′ and 3′ untranslated regions (′-UTR) of MNSV in the presence of purified eIF4E from melon.
Luciferase activity resulting from *in vitro* translated RNAs from the constructs described above. The *in vitro* transcribed RNAs were translated *in vitro* in wheatgerm extract (WGE) in the presence of increasing quantities of purified Cm-EIF4E protein, and the translation efficiency was determined by measuring the luciferase activity. The vertical axis shows the relative luciferase activity (100% corresponds to the activity of 5′-UTR264-f*luc*-3′-UTR264). On the horizontal axis the six groups correspond to six different constructs, as indicated [5′-Mα5, 5′-UTR-Mα5-f*luc*-plasmid; 3′-Mα5, plasmid-f*luc*-3′-UTR-Mα5; 5′-+3′-Mα5, 5′-UTR-Mα5-f*luc*-3′-UTR-Mα5; 5′-+3′-UTRs-264, 5′-UTR-264-f*luc*-3′-UTR-264; 5′-Mα5 and 3′-264 + Mα5, 5′-UTR-Mα5-f*luc*-3′-UTR-264 with stem loop C (SL C) from MNSV-Mα5]. In each group, all bars from left to right correspond to luciferase activity in the presence of increasing concentrations of purified Cm-EIF4E from susceptible (EIF4ES) or resistant (EIF4ER) melon (0–42 ng), as indicated on the right. Translation efficiency data obtained for 5′- + 3′-UTRs-264 upon the addition of eIF4ER (not shown) were very similar to the data shown in this Figure obtained upon the addition of eIF4ES.

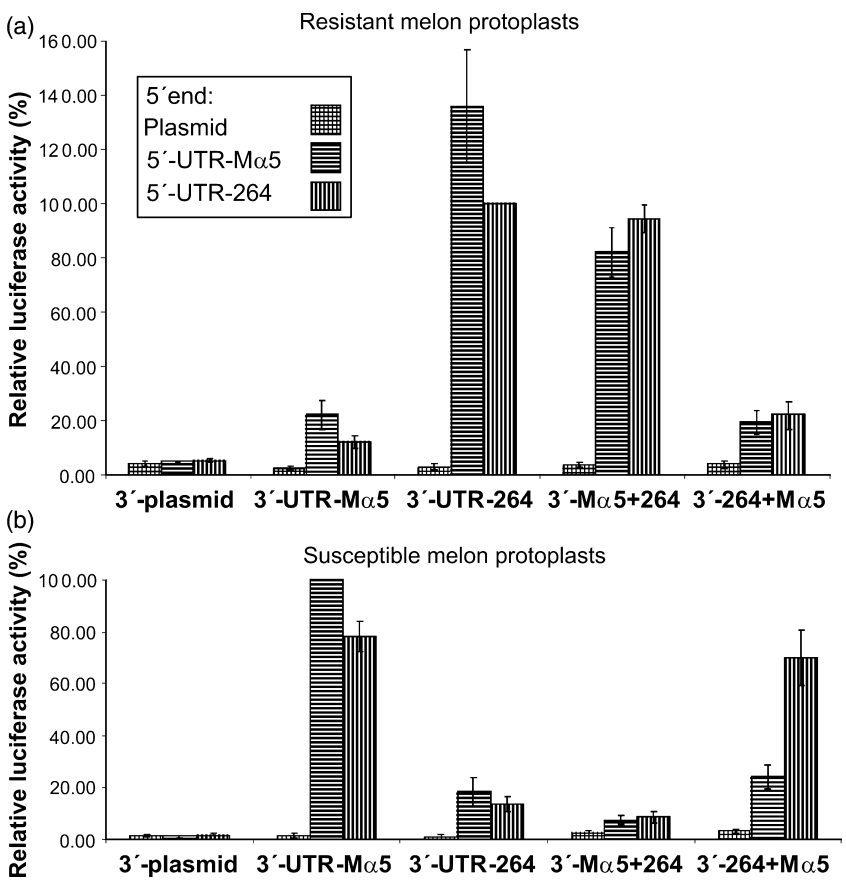

Figure 8. Translation in melon protoplasts of *luc* controlled by the 5′ and 3′ untranslated regions (′-UTRs) of MNSV.
Luciferase activity resulting from the *in vivo* translation of RNAs from constructs described above. The *in vitro* transcribed RNA was electroporated into protoplasts of susceptible or resistant melons, and the translation efficiency was determined by measuring the luciferase activity after a 6-h incubation. The vertical axis shows the relative luciferase activity: 100% corresponds to the activity obtained with 5′-UTR-Mα5-f*luc*-3′-UTRMα5 in susceptible melon, whereas it corresponds to the activity obtained with 5′-UTR264-f*luc*-3′-UTR264 in resistant melon. On the horizontal axis, the five groups shown differ in the sequence present at the 3′ end of *luc*, as indicated. The shading of the bars appearing in each group represent differences in the 5′-end sequences of *luc*, as indicated on the right.
(a) Relative luciferase activities obtained with the constructs indicated in resistant melon protoplasts.
(b) Relative luciferase activities obtained with the same constructs in susceptible melon protoplasts.

The 3′-UTR of MNSV-264 mediates in vivo *cap-independent translation in resistant melon, whereas the 3′-UTR of MNSV-Mα5 does so in susceptible melon*

To study the correlation between cap-independent translation and virulence, the luciferase constructs (Figure 5) were used to transform melon protoplasts and analyse the effects on translation of the MNSV UTRs *in vivo* (Figure 8). In resistant melon protoplasts, translation mediated by the 3′-UTR of MNSV-264 was 28-fold higher than that of the control RNAs (group of columns '3′-plasmid' and first column of group of columns '3′UTR-264'; Figure 8a), whereas

translation mediated by the 3′-UTR of MNSV-Mα5 was only 3.5 times higher (first three groups of columns in Figure 8a). In agreement with the *in vitro* data, the presence of the MNSV 5′-UTR was required *in cis*, and this high cap-independent translational activity was determined by the virulence determinant (group of columns '3′-Mα5 + 264' in Figure 8a). On the other hand, in susceptible melon protoplasts (Figure 8b) the translational activity mediated by the 3′-UTR of MNSV-Mα5 was 60 times higher than that of the control RNAs (groups of columns '3′-plasmid' and '3′-UTR-Mα5' in Figure 8b). In agreement with the complementation experiments described above, the determinant of this increased cap-independent translational efficiency in susceptible melon was MNSV-Mα5 SL C (group of columns '3′-264 + Mα5' in Figure 8b), previously shown to be required for virus viability. The 3′-UTR of MNSV-264 could also enhance cap-independent translation, although only 12-fold compared with the control RNAs (group of columns '3′-UTR-264' in Figure 8b). Therefore, the 3′-UTR of MNSV-264 enhances cap-independent translation in both resistant and susceptible melon, in agreement with the ability of this isolate to infect both melon cultivars.

Discussion

Translation initiation factors of the eIF4E and eIF4G protein families are thought to be universal determinants of plant susceptibility to RNA viruses (Robaglia and Caranta, 2006). However, the molecular mechanisms underlying incompatible virus/host interactions controlled by eIF4E/eIF4G are not yet understood. Here, we show that a 3′-CITE is the virulence determinant in an eIF4E-mediated resistance, allowing us to propose a model for eIF4E-mediated resistance.

Identification of 3′-CITEs in MNSV

For several plant RNA viruses lacking a 5′-cap structure, 3′-CITE sequences have been identified in the 3′-UTR of the genomic RNA (Kneller *et al.*, 2006; Miller and White, 2006). They confer efficient translation initiation at the 5′-proximal AUG. For example, deletion of approximately 100 nt of the start codon BYDV 3′-CITE reduced translation efficiency between 8–20-fold in WGE, and 50–100-fold in barley protoplasts, whereas the addition of a 5′ cap restored translation (Wang *et al.*, 1997). Our results demonstrate that the 3′-UTRs of two different MNSV strains contain sequences that control *in vitro* and *in vivo* cap-independent translation, thus functioning as 3′-CITEs. In WGE, the 3′-UTR of MNSV-264 conferred a ninefold increase in the cap-independent translational efficiency of a reporter gene containing the 5′-UTR of MNSV, whereas this enhancement increased to 28-fold in resistant melon protoplasts. Similarly, the 3′-UTR of MNSV-Mα5 conferred a 3–4-fold increase in cap-independent translational efficiency in WGE supplemented with *Cm*-eIF4ES, and a 60-fold increase in susceptible melon protoplasts. By testing chimeric 3′-UTRs, we showed that the MNSV 3′-CITEs are located in a predicted SL structure, SL C, within the 3′-UTR. The possibility that the 3′-CITE sequence extends into the regions of the 3′-UTR of MNSV-Mα5 and MNSV-264, flanking SL C, being interchangeable, is not probable (but cannot be excluded), as the sequences and secondary structures of the 3′-UTRs of MNSV-Mα5 and MNSV-264 are very different. The sequences and secondary structures of other 3′-CITEs described thus far have been assigned to at least eight structural classes, because most of them bear no similarity to each other in their secondary structure (Miller *et al.*, 2007). Even the two MNSV 3′-CITEs described here bear no obvious resemblance in secondary structure or in sequence, neither to other 3′-CITEs nor to each other, with the exception of the small terminal SL structure exchanged between chimeric constructs Q10 and Q11 (see Figure 4a). Despite this lack of similarity, almost all 3′-CITEs that have been described contain short sequence tracts known or predicted to base-pair to their corresponding 5′-UTRs, a long-distance interaction that is required for cap-independent translation (Miller and White, 2006). For MNSV, we have also shown that the 5′-UTR sequence must be present *in cis* for cap-independent *in vitro* and *in vivo* translation mediated by the 3′-CITEs. Interestingly, the two 5′-UTRs worked with equal efficiency with either 3′-CITE, showing that although a 5′–3′ interaction is necessary for efficient translational initiation, this does not affect the selectivity between resistant and susceptible melon cells. Fabian and White (2004) have proposed 5′–3′ interactions for several viruses belonging to different genera of the *Tombusviridae* family, and also for *Pea stem necrosis virus* (PSNV), which belongs to the same genus as MNSV (*Carmovirus*). Interestingly, the sequence proposed for PSNV-3′-UTR (6 nt) matches part (4 nt) of the sequence in the loop at the end of SL C, which is conserved in all MNSV isolates (see Figure S1). Moreover, a complementary sequence is found in the 5′-UTR for all the MNSV isolates, and our preliminary results suggest that these regions may interact by base-pairing (V.T., unpublished data).

MNSV 3′-CITEs show host specificity

We have shown that *in vivo* cap-independent translation mediated by the 3′-CITE of MNSV-264 was more efficient in resistant melon protoplasts (28-fold increase) than in susceptible ones (12-fold increase), whereas *in vivo* cap-independent translation mediated by the 3′-CITE of MNSV-Mα5 was only efficient in susceptible protoplasts (60-fold increase). Therefore, the two different MNSV 3′-CITEs appear to enhance cap-independent translation differently, depending on the host. It is important to note here that although MNSV-264 can multiply in plants and protoplasts of resistant and susceptible phenotypes, it accumulates

much more efficiently in resistant ones (Diaz *et al.*, 2004) (V.T., unpublished data). The fact that MNSV-264 multiplies to higher levels in resistant than in susceptible cells may be the result of a less efficient function of its 3′-CITE in susceptible cells. Interestingly, host specificity for 3′-CITEs has been reported before: the 3′-CITE of TCV is necessary for viral accumulation in Hibiscus protoplasts, whereas deletion of the entire 3′-CITE had no effect on virus accumulation in Arabidopsis protoplasts (Li and Wong, 2007). Thus, translation initiation controlled by 3′-CITEs seems to be a key regulatory step, offering a potential explanation for the host ranges of plant viruses.

What determines 3′-CITE specificity? In the case of MNSV, the obvious candidate is Cm-eIF4E, because it mediates resistance/susceptibility to the virus, and our *in vitro* translation experiments support this hypothesis: the 3′-CITE of MNSV-Mα5 enhanced cap-independent translation in WGE only when the extract was complemented *in trans* with purified Cm-eIF4ES (from susceptible melon), and not with Cm-eIF4ER (from resistant melon), suggesting that a potential interaction of the 3′-CITE of MNSV-Mα5 with Cm-eIF4ES was efficient, enhancing cap-independent translation, whereas with Cm-eIF4ER it was inefficient, reducing cap-independent translation. This is particularly appealing, as these versions of Cm-eIF4E differ by just one amino acid (Nieto *et al.*, 2006), suggesting that this residue is essential for direct or indirect interactions between Cm-eIF4E and the 3′-CITE. Direct interactions between 3′-CITEs and translation initiation factors have been shown to occur in two cases: the cap-independent translational enhancer domain of satellite tobacco necrosis virus (STNV) has been shown to interact specifically with eIF4F and eIF(iso)4F, as well as with the cap-binding subunits eIF4E and eIF(iso)4E (Gazo *et al.*, 2004), and the 3′-CITE of BYDV has been shown to bind eIF4F, preferentially interacting with eIF4G, and with this binding correlating with the ability of the BYDV 3′-CITE to facilitate cap-independent translation (Treder *et al.*, 2008). These results and the fact that several 3′-CITEs, when moved to the 5′ terminus of viral RNAs to replace their natural 5′-UTR, still facilitate cap-independent translation *in vitro* (Guo *et al.*, 2000; Meulewaeter *et al.*, 1998), suggest that the 3′-CITEs must be responsible for recruiting the host factors involved in translation, and that through the 5′–3′ interaction these are juxtapositioned with the 5′-UTR. In our case, a direct interaction between the 3′-CITEs of MNSV and Cm-eIF4E might be required for the efficient cap-independent translation of viral RNAs, but this hypothesis still has to be tested.

Mechanism of eIF4E-mediated MNSV resistance in melon

Using chimeric mutants, we have shown that the sequence of the 3′-CITE is essential for the virulent MNSV isolate to break *nsv*-mediated resistance, therefore showing that resistance breaking correlated with the virus ability to carry out cap-independent translation. The presence of a 3′-CITE, of MNSV-Mα5 or MNSV-264, was critical for the viability of chimeric viruses in susceptible melon cells, indicating that if one of the two possibly interacting partners is absent (here the 3′-CITE sequence), or if the interaction between them is inefficient (as in resistant melon), the virus fails to multiply because of the reduction in the cap-independent translation efficiency. Taken together, these results allow us to propose a model for the molecular mechanism of *nsv*-mediated resistance to MNSV in melon, in which the circularization of the viral RNA is achieved by base-pairing through a 5′–3′interaction (Figure 9): in susceptible melon (Figure 9a), an interaction between the 3′-CITE of MNSV-Mα5 and Cm-eIF4ES allows efficient cap-independent translation initiation, whereas in resistant melon this interaction, and hence translation, is inefficient, preventing viral multiplication in resistant melon cells. On the other hand, as shown in Figure 9b, the 3′-CITE of MNSV-264 might interact: (i) either with both versions of Cm-eIF4E, albeit less efficiently with Cm-eIF4ES than with Cm-eIF4ER, as translation was less efficient in susceptible protoplasts, (ii) with a Cm-eIF4E isoform, or (iii) with perhaps another translation initiation factor. In Arabidopsis, there are three different *eIF4E* genes (*AteIF4E1–AteIF4E3*), coding for proteins of the eIF4E subfamily, and one gene for eIF(iso)4E. The diversity of the gene family in other plant species is unknown, but several loci have been identified in most species that have been studied (Robaglia and Caranta, 2006). In the most complete and publicly available melon expressed sequence tag (EST) collection (Gonzalez-Ibeas *et al.*, 2007), we have identified at least three cDNAs containing characteristic features of *eIF4E* genes: two of them belong to the eIF4E and one to the eIF(iso)4E subfamilies. The multiplication of another *Carmovirus*, TCV, that, like MNSV, requires its 5′- and 3′-UTRs for efficient cap-independent translation (Qu and Morris,

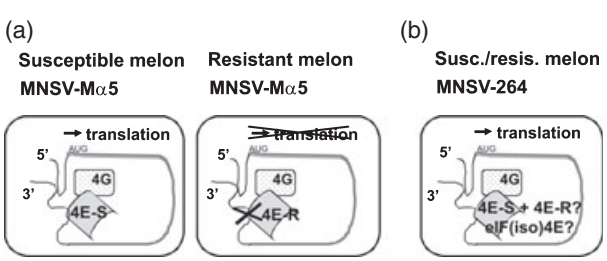

Figure 9. Model for the molecular mechanism of the *nsv* resistance.
(a) Translation initiation of MNSV-Mα5 in susceptible or resistant melon cells: efficient interaction between stem loop C (SL C) and *Cm*-eIF4ES leads to the formation of the translation initiation complex that, through interactions between the 5′-UTR and 3′-UTR of the viral genomic RNA, resulting in its circularization, ends near to the translation start point, thereby allowing the efficient translation of the viral RNA. On the other hand, the inefficient interaction between SL C and *Cm*-eIF4ER avoids the formation of the translation initiation complex and the translation of the viral RNA.
(b) SL C of MNSV-264 might interact with both *Cm*-eIF4Es (S and R), or with an eIF4E isoform or might not require eIF4E for its cap-independent translation in susceptible and resistant melon.

2000), has been shown to be independent of eIF4E1, but dependent on eIF4G (Yoshii *et al.*, 2004). Maybe the translation mechanism of MNSV-264 is similar to that of TCV.

The *nsv*-mediated resistance was expected to provide immunity to MNSV (Diaz *et al.*, 2004), although this resistance has been recently shown to decline at temperatures below 20°C (Kido *et al.*, 2008). This finding might explain why in resistant melon protoplasts, the 3′-CITE of MNSV-Mα5 was still able to mediate some translation (3.5 times higher than the *luc* control construction). The protoplast incubation temperature was 25°C for both multiplication and translation efficiency experiments. As no multiplication of MNSV-Mα5 in resistant melon was observed, this reduced translation efficiency was possibly not enough to guarantee virus multiplication. Thus, the interactions proposed in Figure 9 may be partially temperature dependent. Alternatively, other processes that occur later in the virus cycle may modulate the effect of cap-independent translation initiation. Perhaps the movement of the viral RNA in resistant melon cells could be affected, consistent with observations made for *Pea seed borne mosaic virus* and pea, where eIF4E seems to have a role in cell-to-cell trafficking (Gao *et al.*, 2004).

Experimental procedures

Plants, viruses and virus inoculations

The susceptible (*Nsv*/–) *Cucumis melo* cultivars were the cantaloupe-type accession C-35 ('La Mayora' germplasm collection, Málaga, Spain) and cv. Amarillo (Seminis Vegetable Seeds, http://www.seminis.com). The resistant *C. melo* cultivar (*nsv/nsv*) was the cantaloupe-type accession C-46 ('La Mayora' collection). MNSV isolates were MNSV-264 (Diaz *et al.*, 2002) and MNSV-Mα5 (Diaz *et al.*, 2003). MNSV was maintained and propagated in *C. melo* cotyledons. Inoculation with *in vitro* transcribed RNA from the infectious clones and the chimeric MNSV mutants was performed as described by Diaz *et al.* (2003, 2004). Plants were grown and maintained after inoculation in a greenhouse with a 16-h photoperiod, a day/night temperature of 25°C/18°C and a day/night relative humidity of 70/60%.

Construction and analysis of mutant viruses

Mutant and chimeric viruses were generated as cDNA clones by PCR using the high-fidelity PCR system (Roche, http://www.roche.com). All constructs were verified by sequencing. DNA fragments corresponding to the MNSV genome from pTOPO-264 and pTOPO-264/3′-Mα5 (Diaz *et al.*, 2003, 2004), including the T7 RNA polymerase promoter immediately in front of the 5′ end of the viral genome, were inserted into pBSK+, resulting in pBSK+-264 and pBSK+-264/3′-Mα5. MNSV-264 mutants with truncated versions of ORF X were prepared by site-directed mutagenesis using the Megaprimer method (Diaz *et al.*, 2003, 2004), at the positions identified in Figure 1, followed by directional cloning into *Hpa*I/*Pst*I sites of pBSK+-264.

The chimeric mutants were constructed by amplifying the corresponding fragments (with chimeric primers) using the Megaprimer method, and were then inserted into the *Hpa*I/*Pst*I sites of the corresponding pBSK+-MNSV plasmid (pBSK+-264 when regions of the 3′-UTR of MNSV-264 were exchanged with the corresponding regions of MNSV-Mα5, and pBSK+-264/3′-Mα5 when regions of the 3′-UTR of MNSV-Mα5 were exchanged with the corresponding regions of MNSV-264). Therefore, all mutants had the same MNSV-264 genetic background, except for their chimeric 3′-UTRs.

In vitro transcribed RNA from the above constructs, linearized with *Pst*I, was either inoculated mechanically onto cotyledons or electroporated into protoplasts from resistant and susceptible melon plants. The appearance of necrotic lesions was recorded after visual inspection. The ability of mutants to multiply in melon protoplasts was studied by northern blot; each experiment was carried out at least three times. The last 600 nt from the 3′ end of progeny virus genomes was amplified by RT-PCR (Reverse transcriptase and High-fidelity PCR system; Roche) and sequenced.

Prediction of secondary structures

The 3′-end sequence of seven new MNSV isolates was determined (GenBank accession numbers EU589616–EU589622). The isolates were biologically cloned from infected field samples of melon, cucumber and watermelon plants grown at Almería (Spain) through serial passages in melon at high inoculum dilutions. Total RNA was extracted from MNSV-infected plants using TRI reagent (Sigma-Aldrich, http://www.sigmaaldrich.com). The viral 3′ end was amplified by RT-PCR and the resulting cDNA was sequenced. The primers used were MA196 (5′-gttgttgttgggcggg-3′), containing the last 7 nt of the 3′-UTR conserved between different viral isolates (MNSV-264, MNSV-Mα5 and MNSV-Dutch) and MA245 (5′-actgggggcaatattggtg-3′), located in the *CP* gene.

Computational secondary structure predictions were performed with the program RNAALIFOLD (Hofacker *et al.*, 2002), which combines the use of multiple sequence alignments with free energy minimization data. The prediction of the structure of the virulent MNSV isolates was performed with a sequence alignment including MNSV-264, MNSV-Pα54 and MNSV-264 mutants constructed in the previous section to exclude the presence of ORF X. Additional predictions were performed using PFOLD (Knudsen and Hein, 2003), KNETFOLD (Bindewald and Shapiro, 2006), MFOLD (Zuker, 2003), RNAFOLD (Mathews *et al.*, 1999) and RNASTRUCTURE (Mathews *et al.*, 2004).

Luc constructs

The T7 promoter of pGEM®-T Easy (Promega, http://www.promega.com) included in the *Nae*I/*Nco*I fragment was inserted into the *Sma*I/*Nco*I site of pGL3 (Promega), resulting in the T7-luc plasmid. The MNSV 5′-UTRs (nt 1–87) were amplified from the infectious clones (Diaz *et al.*, 2003, 2004) by PCR using a primer that contained the T7 promoter sequence directly in front of the 5′-UTR sequence, and were directionally cloned into the *Kpn*I/*Nco*I sites of the T7-luc plasmid. The 3′-UTRs were directionally cloned after PCR amplification into the *Xba*I/*Hpa*I sites of the T7-luc plasmid. The *Bsm*I-linearized plasmids were transcribed *in vitro* in the presence or absence of a cap analogue using AmpliScribe™ and Amplicap™ T7-transcription kits (Epicentre Biotechnologies, http://www.epibio.com). Control RNA was synthesized by transcription using the T7-luc plasmid, resulting in a sequence of 38 nt in front of the *luc* start codon. As the T7-luc plasmid was linearized with *Bsm*I, in the absence of a 3′-UTR the *luc* stop codon was followed by 83 nt of the plasmid sequence.

In vitro *translation in wheatgerm extract.* We translated 1.2 μg (14 pmol) of *in vitro* transcribed RNA in WGE (Wheat Germ

Extract Plus, Promega) in a final volume of 8.4 μl following the manufacturer's protocol, incubating at 25°C for 2 h. The reactions were stopped by adding the same volume of 2xCCLR (Promega). The luciferase activity of 4 μl was measured in a luminometer (GloMax™ 20/20). If indicated, purified Cm-eIF4E protein (0–10 pmol) from susceptible or resistant melon was added to the *in vitro* translation reaction. The *in vitro* translation experiments were carried out at least five times for each construct. For complementation experiments, *Cm*-eIF4E was purified as described (Nieto *et al*., 2006).

In vivo *translation in melon protoplasts*

We electroporated 10 μg of *in vitro* transcribed RNA into 1×10^6 protoplasts of susceptible or resistant melons (Diaz *et al*., 2004). To minimize the variations between samples, 2 μg of capped *Renilla* luciferase reporter RNA was introduced along with the virus RNA. The control RNA was obtained from a modified pRL-null vector (Promega) including a poly(A-30)-tail. After 6 h of incubation in the dark at 25°C, protoplasts were lysed in PLB (Promega). *Firefly* and *Renilla* luciferase activities were measured with the Dual-Glo™ Luciferase assay system (Promega). These experiments were carried out at least five times for each construct.

Acknowledgements

This work was supported by grants from Ministerio de Educación y Ciencia (Spain) (AGL2006-08069/AGR) and Fundación Séneca (Región de Murcia, Spain) (05702/PI/07). DGI was a recipient of a predoctoral fellowship from Ministerio de Educación y Ciencia (Spain). We want to thank Christian Clepet (Unité de Recherche en Génomique Végétale, Evry Cedex, France) for his help in purifying Cm-eIF4E, A. Rakotondrafara for her help with the luciferase assays, and Mari Carmen Montesinos and Blanca Gosalvez for their excellent technical assistance.

Supporting Information

Additional Supporting Information may be found in the online version of this article:

Figure S1. Sequence alignment of the 3′-UTRs of 18 MNSV isolates.

Please note: Wiley-Blackwell are not responsible for the content or functionality of any supporting information supplied by the authors. Any queries (other than missing material) should be directed to the corresponding author for the article.

References

Ayme, V., Souche, S., Caranta, C., Jacquemond, M., ChadSuf, J., Palloix, A. and Moury, B. (2006) Different mutations in the genome-linked protein VPg of potato virus Y confer virulence on the pvr23 resistance in pepper. *Mol. Plant-Microbe Interact.* **19**, 557–563.

Bindewald, E. and Shapiro, B.A. (2006) RNA secondary structure prediction from sequence alignments using a network of k-nearest neighbor classifiers. *RNA*, **12**, 342–352.

Borgstrom, B. and Johansen, I.E. (2001) Mutations in pea seedborne mosaic virus genome-linked protein VPg alter pathotype-specific virulence in *Pisum sativum*. *Mol. Plant-Microbe Interact.* **14**, 707–714.

Coudriet, D.L., Kishaba, A.N. and Bohn, G.W. (1981) Inheritance of resistance to muskmelon necrotic spot virus in a melon aphid-resistant breeding line of muskmelon. *J. Am. Soc. Hortic. Sci.* **107**, 789–791.

Diaz, J.A., Nieto, C., Moriones, E. and Aranda, M.A. (2002) Spanish Melon necrotic spot virus isolate overcomes the resistance conferred by the recessive *nsv* gene of melon. *Plant Dis.* **86**, 694.

Diaz, J.A., Bernal, J.J., Moriones, E. and Aranda, M.A. (2003) Nucleotide sequence and infectious transcripts from a full-length cDNA clone of the carmovirus Melon necrotic spot virus. *Arch. Virol.* **148**, 599–607.

Diaz, J.A., Nieto, C., Moriones, E., Truniger, V. and Aranda, M.A. (2004) Molecular characterization of a melon necrotic spot virus strain that overcomes the resistance in Melon and nonhost plants. *Mol. Plant-Microbe Interact.* **17**, 668–675.

Diaz-Pendon, J.A., Truniger, V., Nieto, C., Garcia-Mas, J., Bendahmane, A. and Aranda, M.A. (2004) Advances in understanding recessive resistance to plant viruses. *Mol. Plant Pathol.* **5**, 223–233.

Dreher, T.W. and Miller, W.A. (2006) Translational control in positive strand RNA plant viruses. *Virology*, **344**, 185–197.

Fabian, M.R. and White, K.A. (2004) 5′-3′ RNA-RNA interaction facilitates cap- and poly(A) tail-independent translation of Tomato Bushy Stunt Virus mRNA: a potential common mechanism for Tombusviridae. *J. Biol. Chem.* **279**, 28862–28872.

Fraser, R.S.S. (1990) The genetics of resistance to plant viruses. *Annu. Rev. Phytopathol.* **28**, 179–200.

Fraser, R.S.S. (1999) Plant resistance to viruses. In *Encyclopedia of Virology* (Granoff, A. and Webster, R.G., eds). San Diego CA: Academic press, pp. 1300–1307.

Gao, Z., Johansen, E., Eyers, S., Thomas, C.L., Noel Ellis, T.H. and Maule, A.J. (2004) The potyvirus recessive resistance gene, sbm1, identifies a novel role for translation initiation factor eIF4E in cell-to-cell trafficking. *Plant J.* **40**, 376–385.

Gazo, B.M., Murphy, P., Gatchel, J.R. and Browning, K.S. (2004) A novel interaction of cap-binding protein complexes eukaryotic initiation factor (eIF) 4F and eIF(iso)4F with a region in the 3′-untranslated region of Satellite Tobacco Necrosis Virus. *J. Biol. Chem.* **279**, 13584–13592.

Gonzalez-Ibeas, D., Blanca, J., Roig, C. *et al.* (2007) MELOGEN: an EST database for melon functional genomics. *BMC Genomics*, **8**, 306.

Gordon, K., Futterer, J. and Hohn, T. (1992) Efficient initiation of translation at non-AUG triplets in plant cells. *Plant J.* **2**, 809–813.

Guo, L., Allen, E. and Miller, W.A. (2000) Structure and function of a cap-independent translation element that functions in either the 3′ or the 5′ untranslated region. *RNA*, **6**, 1808–1820.

Hearne, P.Q., Knorr, D.A., Hillman, B.I. and Morris, T.J. (1990) The complete genome structure and synthesis of infectious RNA from clones of tomato bushy stunt virus. *Virology*, **177**, 141–151.

Hibi, T. and Furuki, I. (1985) Melon necrotic spot virus. *CMI/AAB Descriptions of Plant Viruses. No. 302*. Warwick, UK: Association of Applied Biologists

Hofacker, I.L., Fekete, M. and Stadler, P.F. (2002) Secondary structure prediction for aligned RNA sequences. *J. Mol. Biol.* **319**, 1059–1066.

Huang, M., Koh, D.C.-Y., Weng, L.-J., Chang, M.-L., Yap, Y.-K., Zhang, L. and Wong, S.-M. (2000) Complete nucleotide sequence and genome organization of *Hibiscus* chlorotic ringspot virus, a new member of the genus *Carmovirus*: evidence for the presence and expression of two novel open reading frames. *J. Virol.* **74**, 3149–3155.

Kang, B.-C., Yeam, I., Frantz, J.D., Murphy, J.F. and Jahn, M.M. (2005) The pvr1 locus in *Capsicum* encodes a translation initiation factor eIF4E that interacts with Tobacco etch virus VPg. *Plant J.* **42**, 392–405.

Kido, K., Mochizuki, T., Matsuo, K., Tanaka, C., Kubota, K., Ohki, T. and Tsuda, S. (2008) Functional degeneration of the resistance gene nsv against Melon necrotic spot virus at low temperature. *Eur. J. Plant Pathol.* **121**, 189–194.

Kneller, E.L.P., Rakotondrafara, A.M. and Miller, W.A. (2006) Cap-independent translation of plant viral RNAs. *Virus Res.* **119**, 63–75.

Knudsen, B. and Hein, J. (2003) Pfold: RNA secondary structure prediction using stochastic context-free grammars. *Nucleic Acids Res.* **31**, 3423–3428.

Leonard, S., Plante, D., Wittmann, S., Daigneault, N., Fortin, M.G. and Laliberte, J.-F. (2000) Complex formation between Potyvirus VPg and translation eukaryotic initiation factor 4E correlates with virus infectivity. *J. Virol.* **74**, 7730–7737.

Leonard, S., Chisholm, J., Laliberte, J.-F. and Sanfacon, H. (2002) Interaction in vitro between the proteinase of Tomato ringspot virus (genus *Nepovirus*) and the eukaryotic translation initiation factor iso4E from *Arabidopsis thaliana*. *J. Gen. Virol.* **83**, 2085–2089.

Leonard, S., Viel, C., Beauchemin, C., Daigneault, N., Fortin, M.G. and Laliberte, J.F. (2004) Interaction of VPg-Pro of Turnip mosaic virus with the translation initiation factor 4E and the poly(A)-binding protein in planta. *J. Gen. Virol.* **85**, 1055–1063.

Li, W. and Wong, S.-M. (2007) Host-dependent effects of the 3′ untranslated region of turnip crinkle virus RNA on accumulation in *Hibiscus* and Arabidopsis. *J. Gen. Virol.* **88**, 680–687.

Mathews, D.H., Sabina, J., Zuker, M. and Turner, D.H. (1999) Expanded sequence dependence of thermodynamic parameters improves prediction of RNA secondary structure. *J. Mol. Biol.* **288**, 911–940.

Mathews, D.H., Disney, M.D., Childs, J.L., Schroeder, S.J., Zuker, M. and Turner, D.H. (2004) Incorporating chemical modification constraints into a dynamic programming algorithm for prediction of RNA secondary structure. *Proc. Natl Acad. Sci. USA*, **101**, 7287–7292.

Matsuo, K., Kameyi-Iwaka, M. and Ohta, T. (1991) Two new strains of melon necrotic spot virus. *Ann. Phytopathol. Soc. Jpn.* **57**, 558–567.

Meulewaeter, F., Van Montagu, M. and Cornelissen, M. (1998) Features of the autonomous function of the translational enhancer domain of satellite tobacco necrosis virus. *RNA*, **4**, 1347–1356.

Miller, W.A. and White, K.A. (2006) Long-distance RNA-RNA interactions in plant virus gene expression and replication. *Annu. Rev. Phytopathol.* **44**, 447–467.

Miller, W.A., Liu, S. and Beckett, R. (2002) Barley yellow dwarf virus: Luteoviridae or Tombusviridae? *Mol. Plant Pathol.* **3**, 177–183.

Miller, W.A., Wang, Z. and Treder, K. (2007) The amazing diversity of cap-independent translation elements in the 3′-untranslated regions of plant viral RNAs. *Biochem. Soc. Transact.* **035**, 1629–1633.

Moury, B., Morel, C., Johansen, E., Guilbaud, L., Souche, S., Ayme, V., Caranta, C., Palloix, A. and Jacquemond, M. (2004) Mutations in Potato virus Y genome-linked protein determine virulence toward recessive resistances in *Capsicum annuum* and *Lycopersicon hirsutum*. *Mol. Plant-Microbe Interact.* **17**, 322–329.

Nieto, C., Morales, M., Orjeda, G. *et al.* (2006) An eIF4E allele confers resistance to an uncapped and non-polyadenylated RNA virus in melon. *Plant J.* **48**, 452–462.

Qu, F. and Morris, T.J. (2000) Cap-independent translational enhancement of Turnip Crinkle virus genomic and subgenomic RNAs. *J. Virol.* **74**, 1085–1093.

van Regenmortel, M.H.V., Fauquet, C.M., Bishop, D.H.L. *et al.* (2000) *Virus Taxonomy: Seventh report of the International Committee on Taxonomy of Viruses*. San Diego: Academic Press.

Riviere, C.J. and Rochon, D.M. (1990) Nucleotide sequence and genomic organization of melon necrotic spot virus. *J. Gen. Virol.* **71**, 1887–1896.

Robaglia, C. and Caranta, C. (2006) Translation initiation factors: a weak link in plant RNA virus infection. *Trends Plant Sci.* **11**, 40–45.

Rochon, D.M. and Tremaine, J.H. (1989) Complete nucleotide sequence of the cucumber necrosis virus genome. *Virology*, **169**, 251–259.

Schaad, M.C., Anderberg, R.J. and Carrington, J.C. (2000) Strain-specific interaction of the tobacco etch virus NIa protein with the translation initiation factor eIF4E in the yeast two-hybrid system. *Virology*, **273**, 300–306.

Shen, R. and Miller, W.A. (2004) The 3′ untranslated region of tobacco necrosis virus RNA contains a barley yellow dwarf virus-like cap-independent translation element. *J. Virol.* **78**, 4655–4664.

Shirako, Y. (1998) Non-AUG translation initiation in a plant RNA virus: a forty-amino-acid extension is added to the N terminus of the soil-borne wheat mosaic virus capsid protein. *J. Virol.* **72**, 1677–1682.

Treder, K., Pettit Kneller, E.L., Allen, E.M., Wang, Z., Browning, K.S. and Miller, W.A. (2008) The 3′ cap-independent translation element of Barley yellow dwarf virus binds eIF4F via the eIF4G subunit to initiate translation. *RNA*, **14**, 134–147.

Wang, S., Browning, K.S. and Miller, W.A. (1997) A viral sequence in the 3′-untranslated region mimics a 5′ cap in facilitating translation of uncapped mRNA. *EMBO J.* **16**, 4107–4116.

Wittmann, S., Chatel, H., Fortin, M.G. and Laliberte, J.-F. (1997) Interaction of the viral protein genome linked of turnip mosaic potyvirus with the translational eukaryotic initiation factor (iso) 4E of *Arabidopsis thaliana* using the yeast two-hybrid system. *Virology*, **234**, 84–92.

Yoshii, M., Nishikiori, M., Tomita, K., Yoshioka, N., Kozuka, R., Naito, S. and Ishikawa, M. (2004) The Arabidopsis Cucumovirus multiplication 1 and 2 loci encode translation initiation factors 4E and 4G. *J. Virol.* **78**, 6102–6111.

Zuker, M. (2003) Mfold web server for nucleic acid folding and hybridization prediction. *Nucleic Acids Res.* **31**, 3406–3415.

